The multiple spots of the Ganymede auroral footprint

B. Bonfond,[1,2] S. Hess,[3] F. Bagenal,[4] J.-C. Gérard,[1] D. Grodent,[1] A. Radioti,[1]
J. Gustin,[1] and J. T. Clarke[5]

Received 23 August 2013; revised 23 September 2013; accepted 24 September 2013.

[1] The interaction between the moons and the magnetosphere of giant planets sometimes gives rise to auroral signatures in the planetary ionosphere, called the satellite footprints. So far, footprints have been detected for Io, Europa, Ganymede, and Enceladus. These footprints are usually seen as single spots. However, the Io footprint, the brightest one, displays a much more complex morphology made of at least three different spots and an extended tail. Here we present Hubble Space Telescope FUV images showing evidence for a second spot in the Ganymede footprint. The spots separation distance changes as Ganymede moves latitudinally in the plasma sheet, as is seen for the Io footprint. This indicates that the processes identified at Io are universal. Moreover, for similar Ganymede System III longitudes, the distance may also vary significantly with time, indicating changes in the plasma sheet density. We identified a rapid evolution of this distance $\sim$ 8 days after the detection of a volcanic outburst at Io, suggesting that such auroral observations could be used to estimate the plasma density variations at Ganymede. **Citation:** Bonfond, B., S. Hess, F. Bagenal, J.-C. Gérard, D. Grodent, A. Radioti, J. Gustin, and J. T. Clarke (2013), The multiple spots of the Ganymede auroral footprint, *Geophys. Res. Lett.*, *40*, doi:10.1002/grl.50989.

1. Introduction

[2] Io, Europa, Ganymede, and Enceladus are known to generate an auroral footprint on their parent planets [*Bonfond*, 2012, and references therein]. At Jupiter, the magnetic dipole axis is tilted relative to the rotation axis. As a consequence, the plasma of the inner magnetosphere, essentially originating from Io's volcanism, is concentrated along the centrifugal equator which is inclined relative to the satellite's orbital plane. These moons constitute an obstacle for this magnetospheric plasma which is nearly corotating with the planet (see review by *Jia et al.* [2009]). This interaction creates Alfvén waves which are carried away along the magnetic field lines, forming Alfvén wings. It is noteworthy that in a reference frame fixed with the satellite, the Alfvén wings are inclined relative to the magnetic field lines because of the finite velocity of the waves [e.g., *Kivelson et al.*, 2004]. On their path toward the planet, these waves ultimately accelerate electrons which subsequently precipitate into the atmosphere and create auroral emissions [e.g., *Hess and Delamere*, 2012].

[3] The present study focuses on the Ganymede footprint (GFP). Like Io's, the brightness of this footprint appears to be controlled by the location of Ganymede in the plasma sheet [*Bonfond et al.*, 2013; *Hess et al.*, 2013], but it also experiences brightness fluctuations on timescales of 10–40 min and of 1–3 min [*Grodent et al.*, 2009]. Additionally, the size of the spot ($\sim$ 800 km) appears to be consistent with the size of the whole Ganymede magnetosphere rather than the size of the moon itself.

[4] While most footprints are observed as single spots, the Io footprint, the brightest of all footprints, is known to be made of at least three spots and a $< 100°$ longitude long tail. One spot, the main Alfvén wing (MAW) spot, is attributed to electrons being directly accelerated toward Jupiter in the main Alfvén wing. The trans-hemispheric electron beam (TEB) spot is associated with electrons accelerated away from Jupiter in the main Alfvén wing. They form electron beams along the magnetic field lines and cross the equatorial plane and part of them precipitate in the opposite hemisphere, generating the TEB spot. Since these electrons are not slowed down by the dense plasma in the equatorial plane, the TEB spot is found either upstream or downstream of the MAW spot, depending on the centrifugal latitude of Io (see Animation S1 in the supporting information) [*Bonfond*, 2012]. On their way toward Jupiter, the Alfvén waves are partially reflected at the density gradient outside the torus and form a reflected Alfvén wing (RAW). The third spot, always found downstream of the MAW spot, is associated with the electrons accelerated directly toward Jupiter in the RAW (see Animation S2). The tail is believed to be caused either by field aligned quasi-static electric fields powered by the azimuthal acceleration of the quasi-stagnant plasma in Io's wake [*Hill and Vasyliūnas*, 2002; *Ergun et al.*, 2009], or by multiple reflections of the Alfvén waves downstream of Io [*Jacobsen et al.*, 2007; *Bonfond et al.*, 2009].

[5] There is no reason why the Io footprint would be fundamentally different from the others, and it is likely that the other footprints are also made of several spots which have not been identified yet. Here we report the finding of a second spot for the Ganymede footprint, and we characterize its location in order to identify its nature.

2. Image Processing

[6] This study is based on the data set of images of the Jovian aurora acquired between 1997 and 2013 with the

Additional supporting information may be found in the online version of this article.

[1]Laboratoire de Physique Atmosphérique et Planétaire, Université de Liège, Liège, Belgium.
[2]Department of Space Studies, Southwest Research Institute, Boulder, Colorado, USA.
[3]LATMOS, IPSL, CNRS, UVSQ, UPMC, Guyancourt, France.
[4]LASP, University of Colorado Boulder, Boulder, Colorado, USA.
[5]Center for Space Physics, Boston University, Boston, Massachusetts, USA.

Corresponding author: B. Bonfond, Laboratoire de Physique Atmosphérique et Planétaire, Université de Liège, Allée du 6 Août, 17-B5c, BE-4000 Liège, Belgium. (b.bonfond@ulg.ac.be)

0094-8276/13/10.1002/grl.50989

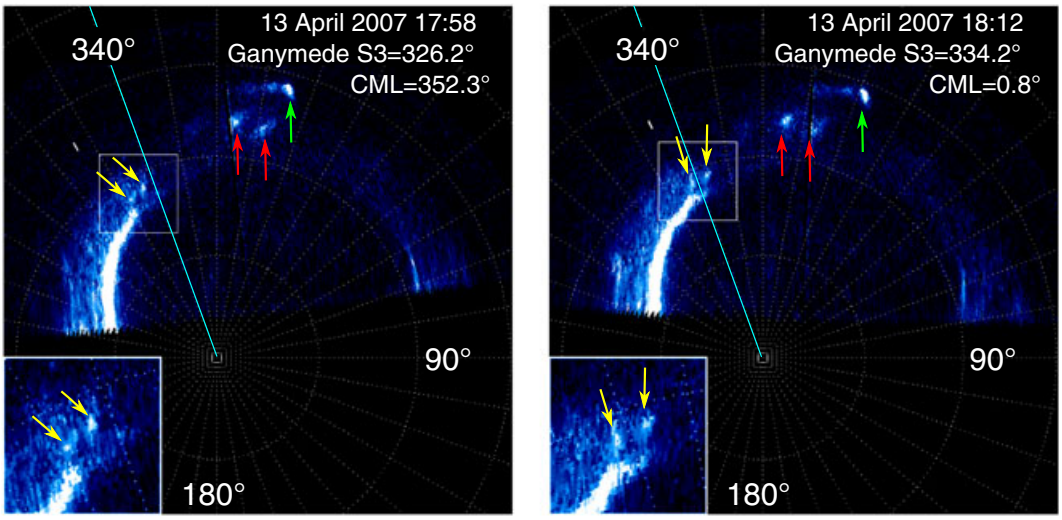

Figure 1. Polar projection of images acquired 14 min apart on 13 April 2007 (see Animation S3). On both images, the Ganymede footprint is made of two spots indicated by the yellow arrows. The green arrow shows the MAW spot of the Io footprint. The red arrows point at two emission patches associated with injection signatures. The spots associated with the footprints moved by $\sim 8°$ of longitude from one image to another while the patches remained approximately fixed.

Far-UV Multi-Anode Microchannel Array channel on the Space Telescope imaging Spectrograph (STIS) and the Solar Blind channel of the Advanced Camera for Surveys (ACS) on board the Hubble Space Telescope (HST). These images were acquired either with the clear and the strontium fluoride filters on STIS or with the F115LP and the F125LP filter on ACS. The platescale is of 0.0248^2 arcsec^2/pixel on STIS and 0.034×0.030 arcsec^2/pixel on ACS, corresponding to ~ 75 and ~ 120 km/pixel, respectively. The point spread function is 2–3 pixels wide on both instruments.

3. Results

3.1. The Nature of the Secondary Spot

[7] Polar projections of the HST images can be rotated so that they are fixed in System III (S3). On such maps, a moving auroral feature located equatorward of the main oval usually denotes the presence of an auroral footprint. On most maps of the southern aurora and possibly on some maps of the northern aurora, two moving spots (typically $> 10\sigma$ above the detection level) can be found close to the foot of the magnetic flux tube passing through Ganymede (Figure 1 and Animations S3–S8). As shown by *Grodent et al.* [2009], the GFP's brightness varies significantly on timescales of minutes. As a consequence, during a given 45 minute long image sequence, a faint spot can significantly dim or even temporarily disappear below the detection threshold (a few kR depending on the background emissions). Its identification is nevertheless made possible by its repeated appearance close to the main GFP spot (i.e., moving similarly relative to the S3 fixed main aurora). However, it also occurs that for a similar longitude range, two spots are observed on one sequence and only one can be seen on another sequence. We suggest that this lack of detection, especially in the north, is probably due to the limited sensitivity of the HST UV cameras.

[8] The distance between these auroral spots varies as a function of the S3 longitude of Ganymede (Figure 2a). More specifically, this distance increases between –60° and 60° and then decreases between 60° and 110°. It also appears to increase again around 150°. If the secondary spot is a RAW spot, then this distance should still decrease to reach a minimum around 200° (Figure 2a (bottom, short-dashed line) and Animation S2), while it should display an opposite behavior for a TEB spot (Figure 2a (bottom, long-dashed line) and Animation S1) [*Bonfond et al.*, 2009]. However, the GFP spots are located close to the limb on the few images showing the footprint around 150°, which increases the uncertainty in their positions and thus on the interspot distances.

[9] Figure 2b shows a sequence of three images acquired on the same day. The S3 longitudes of Ganymede were 61°, 110°, and 145°, respectively. While two spots could be clearly seen on the first and the third images, only one spot is identified on the second one. If the secondary spot is a TEB spot, such a behavior could be interpreted as the merging of the MAW and the TEB spot as Ganymede crosses the centrifugal equatorial plane. However, the lack of detection of the secondary spot could also result from dim emissions below the detection limit.

[10] As seen in Figure 2, the maximum distance between the spots is 4300 km. As the southern GFP footpath is ~115,300 km long, this shift corresponds to $\sim 13°$ of longitude. The Alfvén propagation time from Ganymede ranges from $T_{\min} \approx 140$ to $T_{\max} \approx 1060$ s and is ~ 600 s at 0° centrifugal latitude (see the supporting information). In a frame fixed with Ganymede, the plasma corotates with Jupiter in ~10 h, i.e., with an angular velocity $\Omega = 0.01°$/s. If the interaction is linear [*Jacobsen et al.*, 2007], the maximum distance between the MAW spot and the TEB spot should theoretically correspond to

$$(T_{\max} - T_{\min})\Omega \approx 10°.$$

[11] The time difference roughly corresponds to the time required by the Alfvén waves to cross the plasma sheet from one side to the other. In the case of a RAW spot, the Alfvén waves have to cross the plasma sheet twice so the maximum

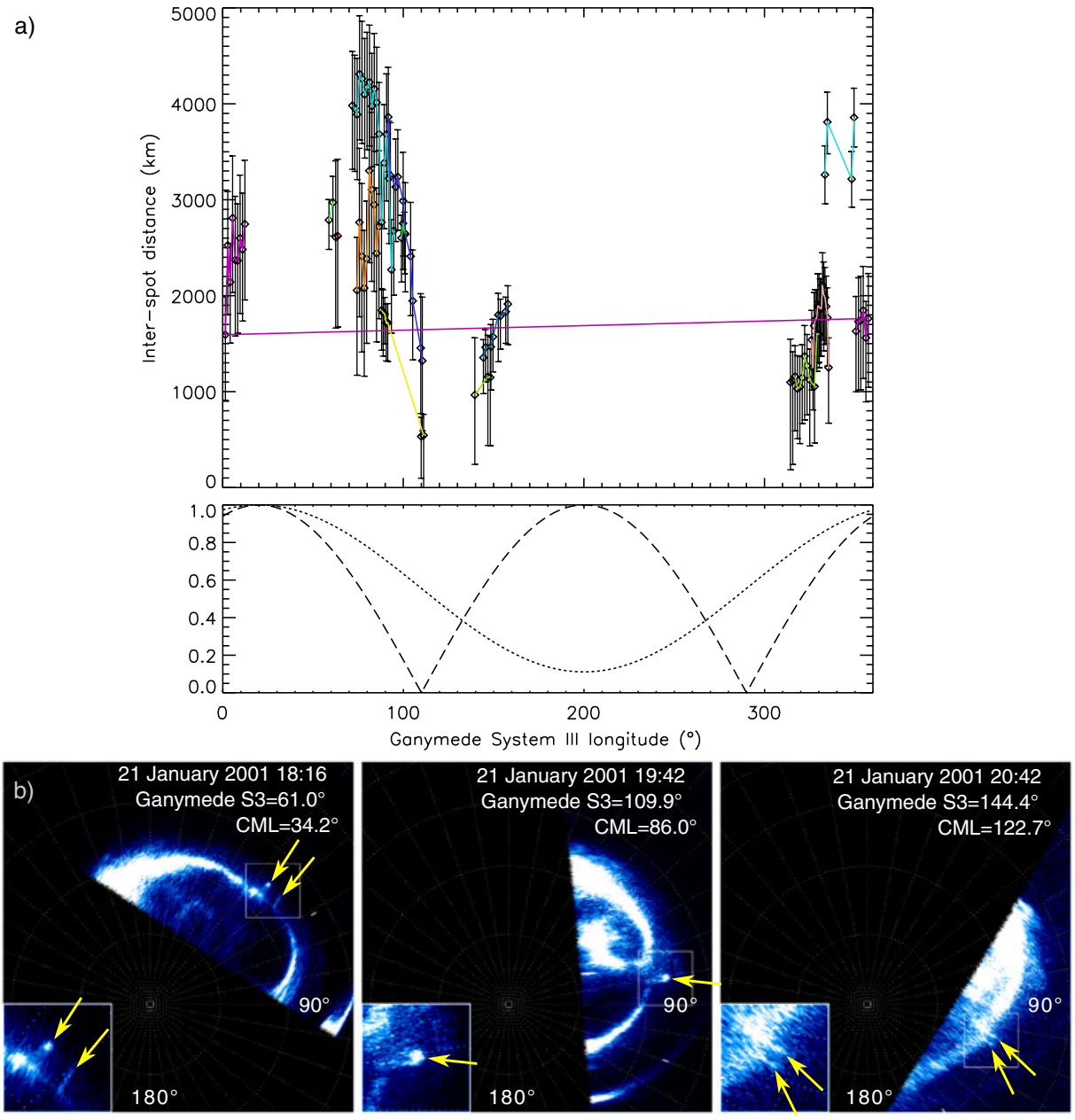

Figure 2. (a) Interspot distance between the two spots of the Ganymede footprint. (top) The colored lines connect points from the same HST orbit. The error bars assume a selection uncertainty of 1 pixel for the first spot and 2 pixels for the second one. (bottom) The long-dashed lines show the expected dependence of the distance for a trans-hemispheric electron beam spot (arbitrary units). In this case, the two spots merged as Ganymede crossed the centrifugal equator. The short-dashed line shows the expected behavior of the distance for a reflected Alfvén wing spot. In this case, the minimum distance is expected when Ganymede is at its northernmost centrifugal latitude ($\sim$ 200° S3). (b) Polar projections of three images acquired on 21 January 2001 at 18:16, 19:42, and 20:42 UT, respectively (see Animation S4). Two GFP spots can be identified on the first and the third images, as Ganymede was either south or north of the centrifugal equator, respectively. Only one spot is visible on the second image, as Ganymede was close to the centrifugal equator.

longitudinal shift should be $\sim$ 20°, which is much larger than observed.

3.2. Plasma Sheet Density Variations

[12] As mentioned before, the Ganymede footprint has been repetitively observed in configurations where the Ganymede S3 longitude was quasi-identical. For example, Figure 3a shows two polar projections of images acquired on 20 February 2007 and 24 May 2007, respectively. Each image is part of a series of 19 images acquired during the same HST orbit, and in both cases, the global trend is a decrease of the interspot distance. However, in the February image, the distance is twice as small as the one from May (2400 km compared to 4300 km). A 450 km equatorward shift of the first spot is also noticeable. Such a shift represents $\sim$ 0.4° of latitude and is smaller (but on the same order of magnitude) than the GFP location shifts already published [*Grodent et al.*, 2008a; *Bonfond et al.*, 2012]. A

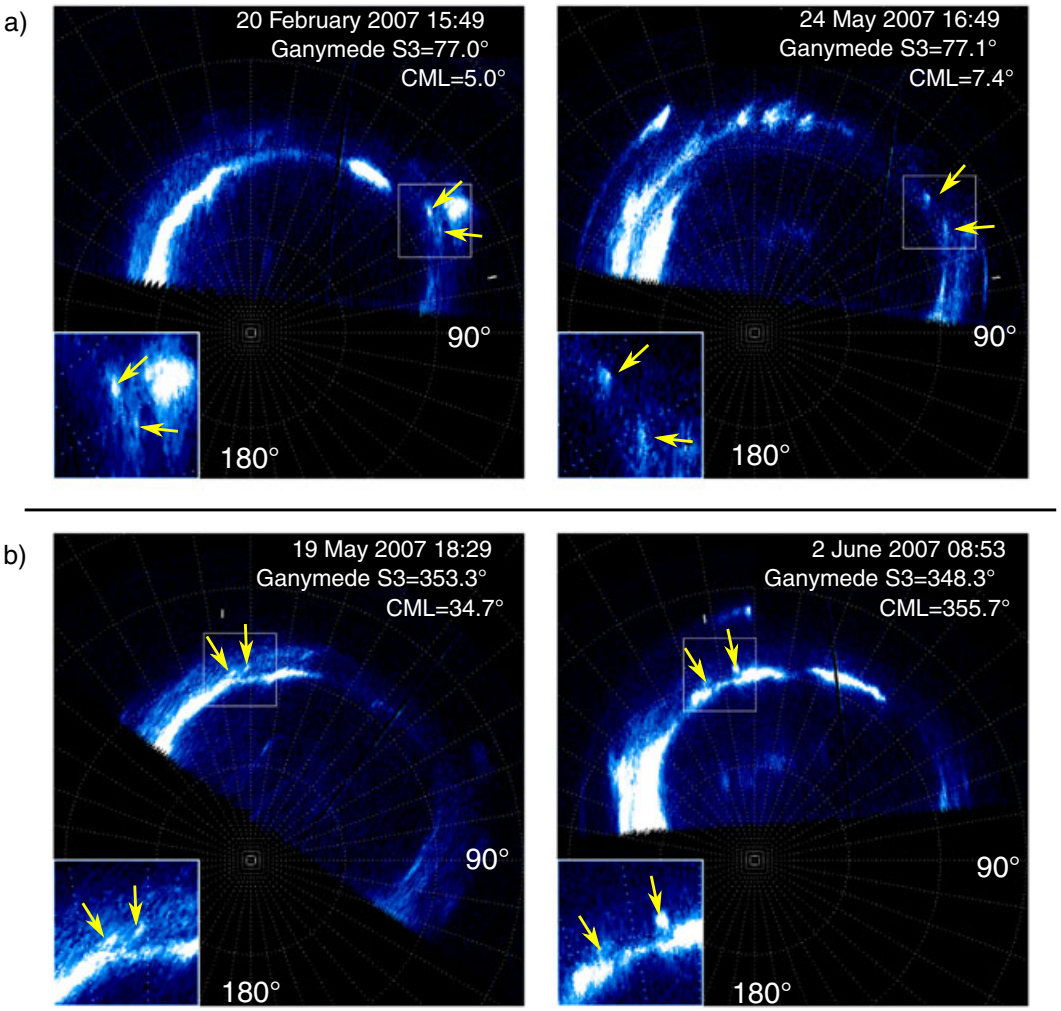

Figure 3. (a) Polar projection of images acquired in very similar configurations (see Animations S5 and S6). Despite the fact that the Ganymede System III longitude is quasi-identical in both cases, significantly different interspot distances were observed. (b) Polar projections of images acquired in relatively similar configurations before and after the iogenic outburst peaking on 30 June 2007 [*Yoneda et al.*, 2009, 2013] (see Animations S7 and S8). The increase of the interspot distance on 2 June 2007 could be related to this event.

possible explanation for both the larger interspot distance and the shift is that the plasma sheet density significantly increased between these two observations. Whatever the nature of the secondary spot, the interspot distance is directly related to the delay between the arrival time of Alfvén waves launched in opposite directions. Since a denser plasma sheet increases the Alfvén propagation time, it also directly increases the interspot distance. Additionally, a denser current sheet further stretches the magnetic field lines, leading to a more equatorward mapping of the GFP [*Grodent et al.*, 2008b]. Moreover, such a behavior could be related to the progressive expansion of the main auroral oval, which has been observed during the same epoch and which has been attributed to an increased mass outflow rate [*Bonfond et al.*, 2012]. These events may be related as an increase of the iogenic plasma input very likely leads to simultaneous increases of the magnetospheric plasma density and of the radial mass outflow rate.

[13] Another example of comparison between images at similar longitudes can be seen in Figure 3b. These images have been acquired on 19 May 2007 and 2 June 2007, respectively. The central meridian longitude (CML; 34.7° compared to 355.7°) and Ganymede's longitude (353.3° compared to 348.3°) are not as similar as in the first example, but these two images of the southern aurora have been obtained right before and after the spectacular sodium nebula brightening of 30 May 2007 [*Yoneda et al.*, 2009]. Concurrently with this enhancement, the intensity of the hectometric (HOM) radio emissions unrelated to the solar wind significantly decreased [*Yoneda et al.*, 2013]. On the first image, the spots are 1700 km apart, while on the second one, the gap reaches 3200 km. For these longitudes, Ganymede is essentially outside the plasma sheet, and the southward going Alfvén waves are relatively unaffected by plasma sheet density variations. However, the northward going Alfvén waves generating the TEB spot and the RAW spot in the southern aurora have to cross the plasma sheet once or twice, respectively. An increase of the plasma sheet density is thus a very plausible explanation for the observed behavior. The time interval between the beginning of the

sodium outburst (25 May) [*Yoneda et al.*, 2009] and its likely consequence at Ganymede (2 June) is $\sim$ 8 days. *Bagenal and Delamere* [2011] estimated the radial transport time from Io to Ganymede to range between 11 and 60 days. Acknowledging that the increase of the plasma supply could precede the detection of the sodium outburst by a couple of days [*Yoneda et al.*, 2010], our result is thus fairly consistent with the lowest value.

4. Conclusions

[14] A second GFP spot is quasi-systematically observed in the southern hemisphere and occasionally seen in the northern hemisphere. The spacing of these spots evolves with the S3 longitude of Ganymede, reaching a maximum of 13°. This longitudinal shift corresponds to a single crossing of the current sheet, which suggests that the second spot is caused by a trans-hemispheric electron beam, by analogy with the Io case. This conclusion is strengthened by the fact that the interspot distance appears to increase around 150° S3, in accordance with expectations for a TEB spot. Further evidence is the identification of either very close spots or only a unique spot around 110° S3. Again, this behavior matches the expectations for a TEB spot, as the main and TEB spots are expected to merge and then separate again as Ganymede crosses the centrifugal equator. Together, these three pieces of evidence strongly suggest that the bidirectional electron acceleration process related to dispersive Alfvén waves [*Jones and Su*, 2008; *Hess et al.*, 2010] is also at play at Ganymede and is thus likely a typical consequence of the satellite-magnetosphere interactions.

[15] The large HST image database acquired during spring 2007 allows us to compare observations acquired in very similar configurations at different times. For all the cases from this campaign, for a given S3 longitude, the interspot distance increased with time. One could possibly relate this behavior with the progressive expansion of the main auroral oval which took place in the same period [*Bonfond et al.*, 2012]. Both phenomena could be a consequence of an enhanced mass output from Io, which would increase both the plasma density and the mass outflow rate. Indeed, $\sim$ 8 days separated the start of the sodium outburst [*Yoneda et al.*, 2013] and the increase of the interspot distance in early June 2007. Additionally, the time interval between the outburst and the disruption of the HOM radio emissions is < 13 days long [*Yoneda et al.*, 2013]. These numbers are consistent with the lowest estimates of the radial transport time from Io to Ganymede (11 days) [*Bagenal and Delamere*, 2011].

[16] As a consequence, the interspot distance of the different footprints could be a valuable proxy for assessing the density of the plasma sheet based on images of the aurora (from Juno, for example). However, simultaneous observations of both the aurora and the plasma torus/plasma sheet could be useful to calibrate the method and assess the effect of nonlinearities in the far-field satellite-magnetosphere interaction [*Jacobsen et al.*, 2007].

[17] **Acknowledgments.** B.B., J.-C.G., D.G., and J.G. were supported by the PRODEX program managed by ESA in collaboration with the Belgian Federal Science Policy Office. B.B. and A.R. were funded by the Fund for Scientific Research (F.R.S-FNRS). J.C. was supported by NASA grants HST-60-11649.01-A and HST-60-10862.01-A from STScI to Boston University. This research is based on observations made with the Hubble Space Telescope obtained at the Space Telescope Science Institute, which is operated by AURA Inc.

[18] The Editor thanks two anonymous reviewers for their assistance in evaluating this paper.

References

Bagenal, F., and P. A. Delamere (2011), Flow of mass and energy in the magnetospheres of Jupiter and Saturn, *J. Geophys. Res.*, *116*, A05209, doi:10.1029/2010JA016294.

Bonfond, B. (2012), When moons create aurora: The satellite footprints on giant planets, in *Auroral Phenomenology and Magnetospheric Processes: Earth And Other Planets*, edited by A. Keiling et al., pp. 133–140, AGU, Washington, D.C., doi:10.1029/2011GM001169.

Bonfond, B., D. Grodent, J.-C. Gérard, A. Radioti, V. Dols, P. A. Delamere, and J. T. Clarke (2009), The Io UV footprint: Location, interspot distances and tail vertical extent, *J. Geophys. Res.*, *114*, A07224, doi:10.1029/2009JA014312.

Bonfond, B., D. Grodent, J.-C. Gérard, T. Stallard, J. T. Clarke, M. Yoneda, A. Radioti, and J. Gustin (2012), Auroral evidence of Io's control over the magnetosphere of Jupiter, *Geophys. Res. Lett.*, *39*, L01105, doi:10.1029/2011GL050253.

Bonfond, B., S. Hess, J.-C. G. D. Grodent, A. Radioti, V. Chantry, J. Saur, S. Jacobsen, and J. Clarke (2013), Evolution of the Io footprint brightness I: Far-UV observations, *Planet. Space Sci.*, doi:10.1016/j.pss.2013.05.023.

Ergun, R. E., L. Ray, P. A. Delamere, F. Bagenal, V. Dols, and Y.-J. Su (2009), Generation of parallel electric fields in the Jupiter-Io torus wake region, *J. Geophys. Res.*, *114*, A05201, doi:10.1029/2008JA013968.

Grodent, D., B. Bonfond, J.-C. Gérard, A. Radioti, J. Gustin, J. T. Clarke, J. Nichols, and J. E. P. Connerney (2008a), Auroral evidence of a localized magnetic anomaly in Jupiter's northern hemisphere, *J. Geophys. Res.*, *113*, A09201, doi:10.1029/2008JA013185.

Grodent, D., J.-C. Gérard, A. Radioti, B. Bonfond, and A. Saglam (2008b), Jupiter's changing auroral location, *J. Geophys. Res.*, *113*, A01206, doi:10.1029/2007JA012601.

Grodent, D., B. Bonfond, A. Radioti, J.-C. Gérard, X. Jia, J. D. Nichols, and J. T. Clarke (2009), Auroral footprint of Ganymede, *J. Geophys. Res.*, *114*, A07212, doi:10.1029/2009JA014289.

Hess, S. L. G., and P. A. Delamere (2012), Satellite-induced electron acceleration and related auroras, in *Auroral Phenomenology and Magnetospheric Processes: Earth And Other Planets*, edited by A. Keiling et al., pp. 295–304, AGU, Washington, D.C., doi:10.1029/2011GM001175.

Hess, S., B. Bonfond, V. Chantry, J.-C. Gérard, D. Grodent, S. Jacobsen, and A. Radioti (2013), Evolution of the Io footprint brightness II: Modeling, *Planet. Space Sci.*, doi:10.1016/j.pss.2013.08.005.

Hess, S. L. G., P. Delamere, V. Dols, B. Bonfond, and D. Swift (2010), Power transmission and particle acceleration along the Io flux tube, *J. Geophys. Res.*, *115*, A06205, doi:10.1029/2009JA014928.

Hill, T. W., and V. M. Vasyliūnas (2002), Jovian auroral signature of Io's corotational wake, *J. Geophys. Res.*, *107*, 1464, doi:10.1029/2002JA009514.

Jacobsen, S., F. M. Neubauer, J. Saur, and N. Schilling (2007), Io's nonlinear MHD-wave field in the heterogeneous Jovian magnetosphere, *Geophys. Res. Lett.*, *34*, L10202, doi:10.1029/2006GL029187.

Jia, X., M. G. Kivelson, K. K. Khurana, and R. J. Walker (2009), Magnetic fields of the satellites of Jupiter and Saturn, *Space Sci. Rev.*, *152*, 271–305, doi:10.1007/s11214-009-9507-8.

Jones, S. T., and Y.-J. Su (2008), Role of dispersive Alfvén waves in generating parallel electric fields along the Io-Jupiter fluxtube, *J. Geophys. Res.*, *113*, A12205, doi:10.1029/2008JA013512.

Kivelson, M. G., F. Bagenal, W. S. Kurth, F. M. Neubauer, C. Paranicas, and J. Saur (2004), Magnetospheric interactions with satellites, in *Jupiter: The Planet, Satellites and Magnetosphere*, edited by F. Bagenal, T. Dowling, and W. McKinnon, pp. 513–536, Cambridge.

Yoneda, M., M. Kagitani, and S. Okano (2009), Short-term variability of Jupiter's extended sodium nebula, *Icarus*, *204*, 589–596, doi:10.1016/j.icarus.2009.07.023.

Yoneda, M., H. Nozawa, H. Misawa, M. Kagitani, and S. Okano (2010), Jupiter's magnetospheric change by Io's volcanoes, *Geophys. Res. Lett.*, *371*, L11202, doi:10.1029/2010GL043656.

Yoneda, M., F. Tsuchiya, H. Misawa, B. Bonfond, C. Tao, M. Kagitani, and S. Okano (2013), Io's volcanism controls Jupiter's radio emissions, *Geophys. Res. Lett.*, *40*, 671–675, doi:10.1002/grl.50095.